# DEPOLARIZATION DIFFUSION DURING WEAK SUPRATHRESHOLD STIMULATION OF CARDIAC TISSUE

Vladimir Nikolski, Aleksandre Sambelashvili, and Igor R. Efimov,
Department of Biomedical Engineering, Case Western Reserve University, Cleveland, Ohio 44106-7207, USA
E-mail: ire@cwru.edu

## Abstract

**Background:** The theory of stimulation of cardiac tissue based on virtual electrode (VE) polarization was presented by Wikswo and his group (Wikswo, Biophys. J., 1995). Four basic regimes were distinguished: anodal make, anodal break, cathodal make, and cathodal break. We sought to determine applicability of this theory for near-threshold stimulus intensities.

**Methods:** For the experiments we used fluorescence optical imaging to map virtual electrode polarization at the epicardium of Langendorff-perfused rabbit hearts stained with voltage-sensitive dyes. Unipolar cathodal pacing was applied during diastole via a platinum-iridium electrodes.

**Results:** During near-threshold cathodal make stimulation we found deviations from Wikswo's theory. We observed that after quick virtual electrode polarization activation starts at hyperpolarized regions and then causes a subsequent activation of the depolarized regions. Such an activation pattern appears similar to break activation. The effect of the depolarization diffusion from depolarized to hyperpolarized regions of the VE obtained by us experimentally was confirmed theoretically by 2D active bidomain simulations.

**Conclusions:** For weak near-threshold stimuli the activation pattern does not fit completely into the established model of Roth and Wikswo thus revealing its limitations.

## Introduction

Ability of electric point stimulation to produce a response in excitable tissues [1,2] and induce [3] or terminate [4] arrhythmia in the heart is well known. Yet,

# Report Documentation Page

| Report Date | Report Type | Dates Covered (from... to) |
|---|---|---|
| 25 Oct 2001 | N/A | - |

| | |
|---|---|
| **Title and Subtitle**<br>Depolarization Diffusion During Weak Suprathreshold Stimulation of Cardiac Tissue | **Contract Number** |
| | **Grant Number** |
| | **Program Element Number** |
| **Author(s)** | **Project Number** |
| | **Task Number** |
| | **Work Unit Number** |
| **Performing Organization Name(s) and Address(es)**<br>Department of Biomedical Engineering Case Western Reserve University Cleveland, OH 44106-7207 | **Performing Organization Report Number** |
| **Sponsoring/Monitoring Agency Name(s) and Address(es)**<br>US Army Research, Development & Standardization Group (UK) PSC 802 Box 15 FPO AE 09499-1500 | **Sponsor/Monitor's Acronym(s)** |
| | **Sponsor/Monitor's Report Number(s)** |

**Distribution/Availability Statement**
Approved for public release, distribution unlimited

**Supplementary Notes**
Papers from 23rd Annual International Conference of the IEEE Engineering in Medicine and Biology Society, October 25-28, 2001, held in Istanbul, Turkey. See also ADM001351 for entire conference on cd-rom.

**Abstract**

**Subject Terms**

| | |
|---|---|
| **Report Classification**<br>unclassified | **Classification of this page**<br>unclassified |
| **Classification of Abstract**<br>unclassified | **Limitation of Abstract**<br>UU |

**Number of Pages**
9

the exact mechanisms of electric stimulation have been unknown until a recent discovery of virtual electrode polarization produced by point stimulation [5,9] which results in a peculiar "dog-bone" pattern of positive and negative polarizations. These polarizations of opposite signs are the so-called virtual cathode (VC) and virtual anode (VA). They represent the driving force, which can be mathematically expressed as the activating function [10,11]. The last is governed by two major parameters: the gradient of extracellular electric field and the structural heterogeneity of the heart, both contributing to polarization of the cellular membrane during stimulus. Active ionic properties of the heart, particularly Ca-channels, modulate these polarizations [12].

Dekker [13] demonstrated that both the onset (make) and termination (break) of stimulation of appropriate intensity and duration could produce a propagated response. Roth [14] and Wikswo et al. [9] provided the first mechanistic explanation of the "make" and "break" excitation (ME and BE) based on virtual electrode polarization. They showed that during make stimulation the heartbeat originates at virtual cathode(s) and is delayed at virtual anode(s). In contrast, during BE depolarized regions are unexcitable due to inactivation of sodium channels by the long stimulus. Therefore, during break stimulation the heartbeat originates at virtual anode(s) and is delayed at virtual cathode(s).

The goal of our study was to investigate the mechanisms of stimulation with clinically relevant short stimuli of weak near-threshold intensities.

## Methods

### *Experimental methods*

The experiments were performed on perfused cardiac preparations obtained from New Zealand rabbits (n = 12). The heart was placed onto a Langendorff apparatus, where it was retrogradely perfused with oxygenated modified Tyrode's solution as previously described [15].

The hearts were stained by 0.5 μM of voltage-sensitive dye di-4-ANEPPS. Motion artifacts in optical recordings were suppressed by excitation-contraction uncoupler 2,3-butanedione monoxime (BDM) (15 mM).

The heart was paced at a steady state cycle length of 400 ms at the base of left ventricle with *Basic Pacing Electrode.* Test stimuli were applied with *Test Stimulus Electrode* in the middle of field of view at a coupling interval of 350 ms with amplitude of 0.2-60 mA and duration of 2 ms from a constant current source (A385, WPI). *Recording Electrode* was used to detect the propagated response in order to confirm suprathreshold pacing. Basic pacing stimulus strength was adjusted to twice the diastolic threshold of excitation.

Transmembrane potential (mV) was recorded using a 16x16-element photodiode array (Hamamatsu) with high resolution (252 μm, 343 μs) from the 4x4 mm area near the tip of the test electrode (0.12 mm platinum-iridium Teflon-coated wire) positioned on the epicardium of the left ventricle.

***Numerical methods***

We guided our experiments with theoretical predictions. We reproduced 2-dimensional bidomain model with active kinetics as described by Trayanova and Scoubine [18].

The bidomain model is based on the representation of the cardiac tissue as two interpenetrating extra- and intracellular domains each of them having different conductivities along and across the direction of the fibers [16,17]. The state variables describing the system are intracellular $\phi_i$ and extracellular $\phi_e$ potentials defined everywhere in the domain of interest $\Omega$. The variable of interest is the transmembrane potential defined as a difference $V_m = \phi_i - \phi_e$. The following coupled reaction-diffusion equations constitute the bidomain model:

$$\nabla \cdot (\hat{\sigma}_i \nabla \phi_i) = I_m$$

$$\nabla \cdot (\hat{\sigma}_e \nabla \phi_e) = -I_m - I_0 \qquad \text{in } \Omega$$

where $\hat{\sigma}_i$ and $\hat{\sigma}_e$ are intra- and extracellular conductivity tensors respectively, $I_m$ is the volume density of the transmembrane current, $I_0$ - volume density of the stimulation (shock) current.

The transmembrane current is described as a sum of capacitive, ionic and electroporation currents [18]:

$$I_m = \beta(C_m \frac{\partial V_m}{\partial t} + I_{ion}(V_m, t) + G(V_m, t) \cdot V_m)$$

where $\beta$ - the surface to volume ratio (total membrane area divided by the total tissue volume), $C_m$ - specific membrane capacitance, $G(V_m, t)$ - electroporation conductance. The last is described by empirical equations [18], e.g.:

$$\frac{dG}{dt} = \alpha \exp(\beta(V_m - V_{rest})^2)(1 - \exp(-\gamma(V_m - V_{rest})^2)), \qquad G(0) = G_0$$

Here $\alpha, \beta, \gamma$ are electroporative coefficients, $V_{rest}$ is the resting transmembrane potential. The values of all the parameters are given in Table 1.

As a model of cardiac myocytes we used the original BRDR model [19] modified by Skoubine, Trayanova et. al. in order to accommodate strong electric fields [18].

We used the following boundary conditions

$$\frac{\partial \phi_i}{\partial \vec{n}} = 0 \qquad \phi_e = 0 \text{ on } \partial\Omega$$

For numerical solution of the bidomain system we used a square grid with the space-step $h_x=h_y=0.4$ *mm*, the time step was $\Delta t=0.02$ *ms*. To invert the sparse matrix inversion we employed the Generalized Minimum Residual (GMRES) method [20,21] as the most robust and fast for our case. We used diagonal preconditioning for this method. Calculations were performed on Dell Pentium III PC.

## Results

During excitation by strong anodal and cathodal stimuli at the first 5 ms the anodal wavefront has an elliptical shape elongated along the fibers, while the cathodal wavefront is more rectangular. The activation starts at the positive VE regions with a delayed propagation through hyperpolarized area. These results correspond to those previously obtained by Wikswo et al. for so-called make stimulation.

However, the near-threshold current strength stimulation develops differently. The anodal wavefront is formed in a similar way to the one for the strong stimulus while cathodal activation starts from initially hyperpolarized regions but not from the positive

VE areas (Fig. 1). As a result cathodal wavefront for near threshold stimulus originates and propagates alike an anodal wavefront.

The observed difference in a wavefront formation during strong and near threshold cathodal stimulations remains in the absence of excitation-contraction uncoupler 2,3-butanedione monoxime. Without the uncoupler the pacing threshold is significantly smaller so it is difficult to the see the VE pattern for the near threshold stimulus. Nevertheless the comparison of the initial wavefronts indicates that during the near threshold cathodal stimulation wavefront also starts from the hyperpolarized area of VE.

Computer simulations confirmed our experimental observations. Near-threshold 2 ms stimulus applied to the center of the square sheet of bidomain tissue resulted in virtual electrodes and after termination of the stimulus the wavefront started at the initially hyperpolarized regions. This is illustrated in Fig 2 where two action potentials at two different points of VE are presented. As it can be seen the virtual cathode area depolarizes first. Yet the depolarization is not strong enough for the activation and it diffuses away to the hyperpolarized regions of the virtual anode. Those regions fire in response to the intensive current inflow and then their activation spreads back to the virtual cathodes causing them to fire.

## Conclusions

This work reveals certain limitations to the commonly accepted model of make and break excitation suggested by Wikswo et al. Particularly it shows that for weak stimuli depolarization diffusion leads to a typical break-like excitation pattern for the case when make excitation is expected.

The nature of the ionic mechanisms that underlie the interplay between excitation and depolarization diffusion and their role in wavefront formation still remains obscure.

## References


1. Swammerdam,J. Biblia Naturae. 1738. H.Boerhaave, Leyden.

2. Galvani,L. De vibribus electricitatis in motu musculari. Commentarius. De Bononiesi Scientarium et Ertium Instituto atque Academia Commentarii 7:363-416.

3. Hoffa,M, Ludwig,C. Einige neue Versuche uber Herzbewegung. Zeitschrift Rationelle Medizin 9:107-144.

4. Prevost,JL, Battelli,F. Sur quel ques effets des dechanges electriques sur le coer mammifres. Comptes Rendus Seances Acad Sci 129:1267.

5. Sepulveda,NG, Roth,BJ, Wikswo,JP. Current injection into a two-dimensional anisotropic bidomain. Biophysical Journal 55:987-999.

6. Wikswo JP,Jr, Wisialowski,TA, Altemeier,WA, Balser,JR, Kopelman,HA, Roden,DM. Virtual cathode effects during stimulation of cardiac muscle. Two-dimensional in vivo experiments. Circulation Research 68:513-530.

7. Knisley,SB, Hill,BC, Ideker,RE. Virtual electrode effects in myocardial fibers. Biophysical Journal 66:719-728.

8. Neunlist,M, Tung,L. Spatial distribution of cardiac transmembrane potentials around an extracellular electrode: dependence on fiber orientation. Biophysical Journal 68:2310-2322.

9. Wikswo,JP, Lin,S-F, Abbas,RA. Virtual electrodes in cardiac tissue: a common mechanism for anodal and cathodal stimulation. Biophysical Journal 69:2195-2210.

10. Rattay,F. Ways to approximate current-distance relations for electrically stimulated fibers [published erratum appears in J Theor Biol 1987 Oct 21;128(4):527]. J Theor.Biol. 125:339-349.

11. Sobie,EA, Susil,RC, Tung,L. A generalized activating function for predicting virtual electrodes in cardiac tissue. Biophysical Journal 73:1410-1423.

12. Cheek,ER, Ideker,RE, Fast,VG. Nonlinear changes of transmembrane potential during defibrillation shocks : role of Ca(2+) current. Circ Res 87:453-459.

13. Dekker,E. Direct current make and break thresholds for pacemaker electrodes on the canine ventricle. Circulation Research 27:811-823.

14. Roth,BJ. A mathematical model of make and break electrical stimulation of cardiac tissue by a unipolar anode or cathode. IEEE Trans Biomed Eng 42:1174-1184.

15.Efimov,IR, Cheng,Y, Van Wagoner,DR, Mazgalev,T, Tchou,PJ. Virtual electrode-induced phase singularity: a basic mechanism of failure to defibrillate. Circulation Research 82:918-925.

16. C.S. Henriquez, Simulating the electrical behavior of cardiac tissue using the bidomain model, Crit.Rev.Biomed.Eng. 21 (1993) 1

17. A.L. Muler, V.S. Markin, Electrical properties of anisotropic nerve-muscle syscytia. I. Distribution of the electronic potential, Biofizika 22 (1977) 307.

18. K. Skouibine, N. Trayanova, P. Moore, A numerically efficient model for simulation of defibrillation in an active bidomain sheet of myocardium, Math. Bios. 166 (2000) 85

19. G.W. Beeler, H. Reuter, Reconstruction of the action potential of ventricular myocardial fibers, J. Physiol. 268 (1977) 177.

20.Y. Saad, M.H.Schultz, GMRES: a generalized minimal residual algorithm for solving nonsymmetric linear systems, SIAM J. Sci. Statist. Comput. 7 (1986) 856.

21. Press,WH, Teukolsky,SA, Vetterling,WT, Flannery,BP. Numerical Recipies in C. 1997. Cambridge University Press, Cambridge.

| Parameter | Value |
|---|---|
| $C_m$ | 1.0 $\mu F/cm^2$ |
| $\beta$ | 3000 $cm^{-1}$ |
| $\sigma_{ix}$ | 0.375 $mS/cm$ |
| $\sigma_{iy}$ | 3.750 $mS/cm$ |
| $\sigma_{ex}$ | 2.140 $mS/cm$ |
| $\sigma_{ey}$ | 3.750 $mS/cm$ |
| $\alpha$ | $2.5 \cdot 10^{-3}$ $mS/cm^2 \cdot ms$ |
| $\beta$ | $2.5 \cdot 10^{-5}$ $1/mV^2$ |
| $\gamma$ | $1.0 \cdot 10^{-9}$ $1/mV^2$ |
| $I_0$ | 50 $\mu A/cm^2$ |

**Table 1. 2D active bidomain model parameters**

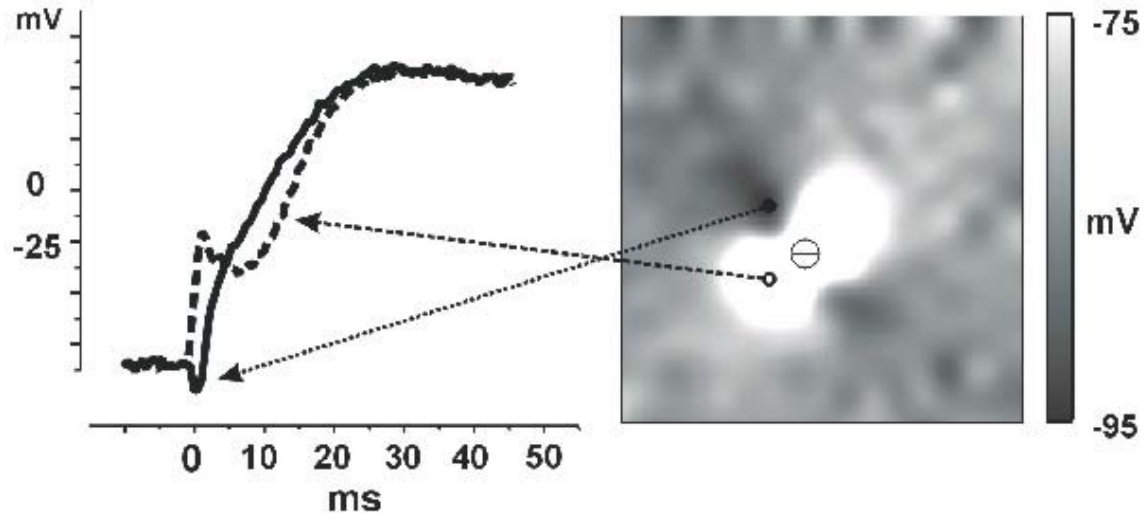


**Fig 1**. Right panel – experimental recording of VE at 2 ms after the near the threshold make cathodal pulse. Left panel - action potential traces from hyper- (solid) and depolarized (dashed) areas. The hyperpolarized regions activate before the depolarized regions.

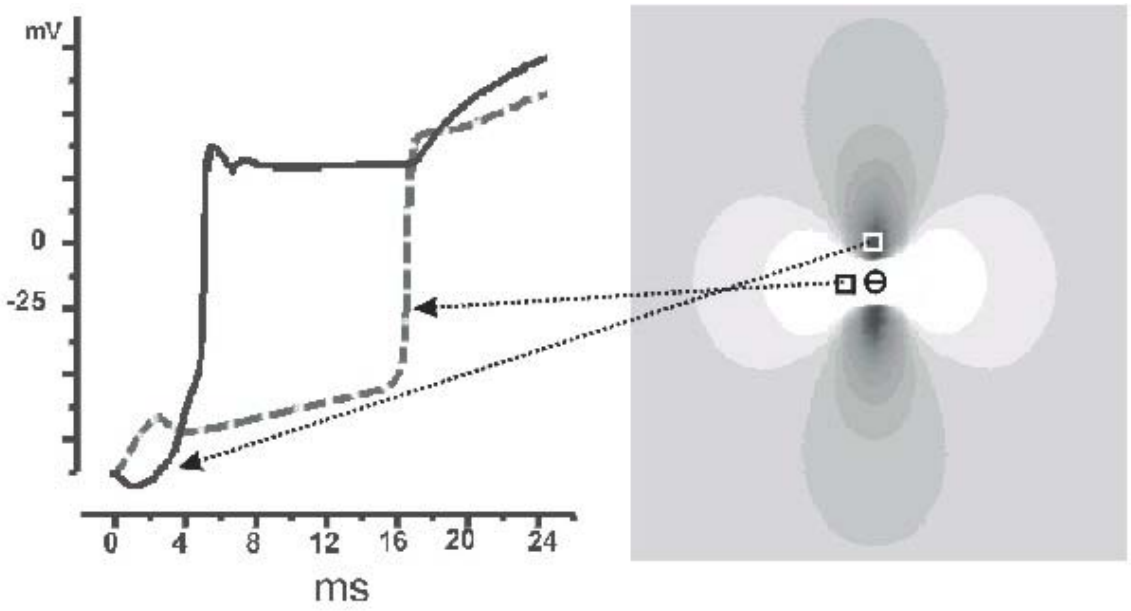


**Fig 2**. Right panel –picture of VE at 2.4 ms after the near the threshold make cathodal pulse obtained from the active bidomain simulation. Left panel - action potential traces from hyper- (solid) and depolarized (dashed) areas. The hyperpolarized regions activate before the depolarized regions.